ENGINEERING TRANSACTIONS • *Engng. Trans.* • **55**, 2, 155–180, 2007
Polish Academy of Sciences • Institute of Fundamental Technological Research

IMPROVEMENT OF HANDLING BY MEANS OF ACTIVE SUSPENSION CONTROL

T. R. O r i[1)], M. N. I c h c h o u[2)], P. P. G b a h a[1)], L. J e z e q u e l[2)]

[1)]**Institut National Polytechnique Houphouët Boigny**
Côte d'Ivoire

[2)]**Ecole Centrale Lyon**
France

Brake systems have become increasingly complex. They must not only slow down or stop a vehicle under extreme conditions within short distances, but also reduce the effort exerted by the driver. This phenomenon is difficult to approach because it depends on the vehicle's architecture. This is why, in this paper, the first part will give the basis for modelling of the complete vehicle including the frame and the tires, in a 3D format. A 2D control law model will be synthesized to obtain the best performances for road behaviour. This control law is based on the theory of Linear Quadratic control (LQ). It is also extended to cover the 3D vehicle model. The last part gives the numerical simulation results which demonstrate the effectiveness of this law for vehicle performances.

Key words: active suspensions, optimal control, brakes, vehicle dynamics, angular dynamics, comfort.

Notations

M_s	rigid body mass of half-car,
$M_{nsv},\ M_{nsr}$	masses respectively of the front axle and the rear axle,
$l_v,\ l_r$	distances from center of gravity to vehicle front wheel, respectively, and to vehicle rear wheel,
I_p	vehicle pitch inertia about center of gravity,
θ	vehicle pitch angle about center of gravity,
h	height of center of gravity from the road,
$z_{sv},\ z_{sr}$	vertical displacements, respectively of the front and the rear of the rigid body,
$\dot{z}_{sv},\ \dot{z}_{sr}$	vertical velocities, respectively of the front and the rear of the rigid body,
$z_{rv},\ z_{rr}$	vertical displacements respectively of the front and rear axle,
$\dot{z}_{rv},\ \dot{z}_{rr}$	vertical velocities, respectively of the front and rear axle,
$z_{tv},\ z_{tr}$	road displacements, respectively on the front and rear wheel,
$k_{sv},\ k_{sr}$	spring constant of the secondary suspensions, respectively front and rear,

$b_{sv},\ b_{sr}$	damping coefficients of the secondary suspensions, respectively front and rear,
$k_{tv},\ k_{tr}$	spring constant of the primary suspensions, respectively front and rear,
$b_{tv},\ b_{tr}$	damping coefficients of the primary suspensions, respectively front and rear,
$f_{av},\ f_{ar}$	friction forces ,respectively of the front and rear wheels,
$f_{zv},\ f_{zr}$	normal forces, respectively of the front and rear wheels,
$u_v,\ u_r$	active control forces, respectively of the front and rear wheels,
$x, \dot{x},\ \ddot{x}$	position, velocity and acceleration of the vehicle,
$w_{av},\ w_{ar}$	angular velocity, respectively of the front and rear wheels,
$\dot{w}_{av},\ \dot{w}_{ar}$	angular acceleration, respectively of the front and rear wheels,
$T_{bv},\ T_{br}$	front and rear disc brake torque, respectively,
$J_v,\ J_r$	inertias, respectively of the front and rear wheels,
r	effective tyre radius,

1. Introduction

Many theoretical and experimental works propose applications of optimal control theories for the active control of mechanical systems and structures vibrations. Several works, such as those of Karnopp [1, 2, 3], in the field of vehicle suspensions have made it possible to show the performances obtained by active systems for vehicle comfort and stability improvements.

The interesting results obtained by this type of work on vehicle suspensions led us to raise the question of its possible application to other problems. This study proposes to extend its use to the improvement of road behaviour. During the braking phase for example, there are longitudinal and transverse load transfers, causing pressure loss on certain wheels. It is necessary to add a supplementary load on each unloaded wheel and discharge those which are overloaded. According to the Coulomb law ($T = \mu.N$), if one manages to increase the normal force (N), the force of friction (T) should also increase. That would contribute to adding loads to the discharged wheels and to obtain good deceleration of the vehicle.

For the same purpose, several mechanisms have already been installed on road vehicles. These mechanisms, such as ABS (Anti-lock Braking System) and ESP (Electronic Stability Program), have proved their effectiveness in improving the stopping distance and handling of vehicles. In the braking field, car manufacturers and the scientific community have optimized the parameters of vehicles to obtain effective braking and optimal reduction to the braking distance. Since people drive ever faster, it would be interesting to develop an innovative system adapted to this trend in driver behaviour. This paper offers then a new concept which is able to increase safety and to improve handling, and which could be added to the existing powerful systems (ABS, ESP...).

In this contribution, we propose a method which consists in increasing the friction force between the tire and the road while acting on the suspension.

For this purpose, we use a control law which will act on some of the vehicle degrees of freedom. This action represents the behaviour of an actuator which increases the normal force on the contact surface (between the tyre and the road), and which will affect the frictional forces. A study conducted in France by the car manufacturer Renault, on the circumstances of accidents, revealed that 36% of accidents take place in a straight line, 18% at roads intersections and 46% in curves. The greatest share of accidents occur in curves because of instabilities caused by the action of the driver, or by external actions. Among the instabilities caused by external actions, one can consider two cases. In the first case, the vehicle is in low adherence zone (in a discontinuous manner). A loss can then occur in the tracking forces on one or more tyres, generating instability. In the second case, the vehicle can also be subjected to aerodynamic disturbances, generating an additional yaw motion which could be a source of instability. Concerning instabilities caused by the driver, it corresponds mainly to the situation in which the driver imposes two or several successive changes of direction of the vehicle. This case could occur when trying to avoid an obstacle, a change of lane in an urgent situation or at an intersection in the presence of another vehicle. We will use the latter example in our simulations because the suspensions are strongly strained.

The work offered here uses optimal control features, takes into account the existing knowledge in terms of vehicle dynamics in order to put them in operational form and applicable to the design problem of vehicles. Models were developed to design the control device and to simulate the operation of the system in order to evaluate the law of control. Considering the optimal control principles, we proposed an active control law for various cases of constraints. This law is meant to significantly improve vehicle handling. Simulations were carried out in the braking phase because the vehicle's suspension is also strained when avoiding an obstacle. The paper is organized as follows: Sec. 2 gives basic equations describing the vehicle dynamics. It includes all relevant components description and details. Section 3 discusses deeply the cost functional representing the optimal vehicle in terms of braking capacities and performances. Section 4 offers some numerical simulations and includes main situations in an attempt to check the robustness of the proposed solution. Section 5 concludes the paper.

2. Vehicle Dynamics Model

2.1. Vehicle dynamics concept

To understand the concepts which will be referred to in this paper, we introduce here some elementary notions related to vehicle dynamics. Two reference frames are needed. The first reference frame is related to the road. The second

reference is fixed at the mass center G of the vehicle. We define the angle of rolling as being the rotation around the longitudinal axis (GX), the angle of pitch as being the rotation around the transverse axis (GY) and the angle of yaw, like that of rotation, around the vertical axis (GZ).

It is important to define the variables which will characterize the state of the vehicle. Among them are the parameters which will be useful for the study of contact between the wheel and the ground and those concerning to the tyres. The angle between the tyre and the vertical axis is the steering angle (α) and the angle between the velocity vector and the longitudinal axis is the drift angle (γ).

To simplify and reduce the calculations for asymmetrical braking, we study the dynamic behaviour of a vehicle whose trajectory is circular.

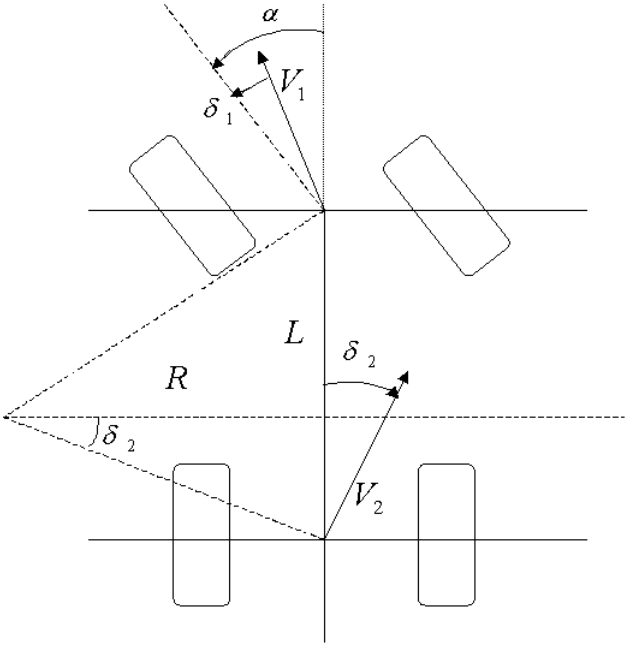

FIG. 1. Angular dynamics.

We assume in this model that the angles between the right wheel and the left wheel of the same axle are identical. δ_1 and δ_2 denote the drift angles of the right axle and the rear axle. δ is the drift angle at the mass center. If we impose a steering angle α, the vehicle runs in a circle whose radius is equal to $R = L/[\alpha - (\delta_2 - \delta_1)]$. If the drift angles of the right axle and the rear axle are known, the behaviour of the vehicle can be predicted. If $(\delta_2 - \delta_1) < 0$, the vehicle is oversteering or if $(\delta_2 - \delta_1) > 0$, the vehicle is understeering. And if $(\delta_2 - \delta_1) = 0$, the vehicle is on the trajectory.

If the vehicle is on a circular trajectory and we accelerate, if it is necessary to add steering to maintain the trajectory, the vehicle is understeering. On the other hand, if it is necessary to decrease steering, then the vehicle is oversteering. And there is a critical velocity beyond which the vehicle becomes unstable. It is necessary in this case to steer right in order to go left. This variation of angle, which characterizes the mode established in turns is called angular dynamics. Angular dynamics can be defined as being the partial derivative of the steering angle compared to transverse acceleration. Under these conditions, the vehicle remains on a circular trajectory of radius R at constant. The angular dynamics is expressed by:

$$da = \frac{d\alpha}{d\gamma_t}$$

where γ_t represents transverse acceleration. The sign of angular dynamics gives then the character of the vehicle. In order to simulate the behaviour of the tyres on a road, it is essential to know their characteristics. We introduce the concept of sliding. Sliding g represents a percentage. If the wheel is blocked and the vehicle is not stopped, then the sliding is equal to – 100%. But if the wheel slips and the vehicle is stopped, then the sliding is equal to 100%. For good adherence, Fig. 2 resulting from Pacejka's tyre model shows that friction force is maximum when sliding is around 10%.

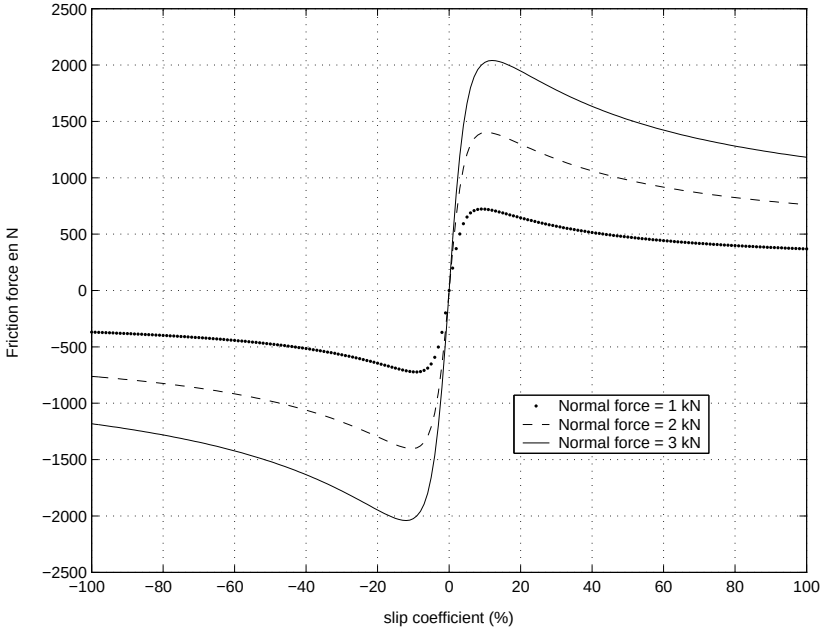

Fig. 2. Friction force according to the slip coefficient.

All the forces of the ground acting on the tyre can be divided into three principal components: F_x represents the trail of braking when the force is opposed to the wheel movement (during braking) or acceleration when it goes in the direction of the movement, F_y is the lateral force of guiding. It is related to the value of pneumatic drifts. F_z is the vertical load which acts on the tyre. It depends on the static weight of the vehicle but also on its dynamic state. It is greatly influenced by the transfers of load during acceleration, braking or curves.

2.2. Model and equations of the vehicle

This model [4, 5] includes the rigid mass of the vehicle's body and the four unsprung masses. It has 22 degrees of freedom, $(x_G,\ y_G,\ z_G,\ \theta,\ \varphi,\ \psi)$ for the vehicle's body, $(x_{ij},\ y_{ij},\ z_{ij})$ for each unsprung mass and (w_{ij}) for each wheel in rotation. We can simulate the dynamic behaviour of a vehicle in real time using this model. Thus, it facilitates experimentation on controlled frame systems using a control simulator, integrating the reactions of a real driver.

The index $i = 1$ is for the front wheel-axle unit, $i = 2$ is the rear wheel-axle unit. The index $j = 1$ is for the left-hand side, and $j = 2$ for the right-hand side.

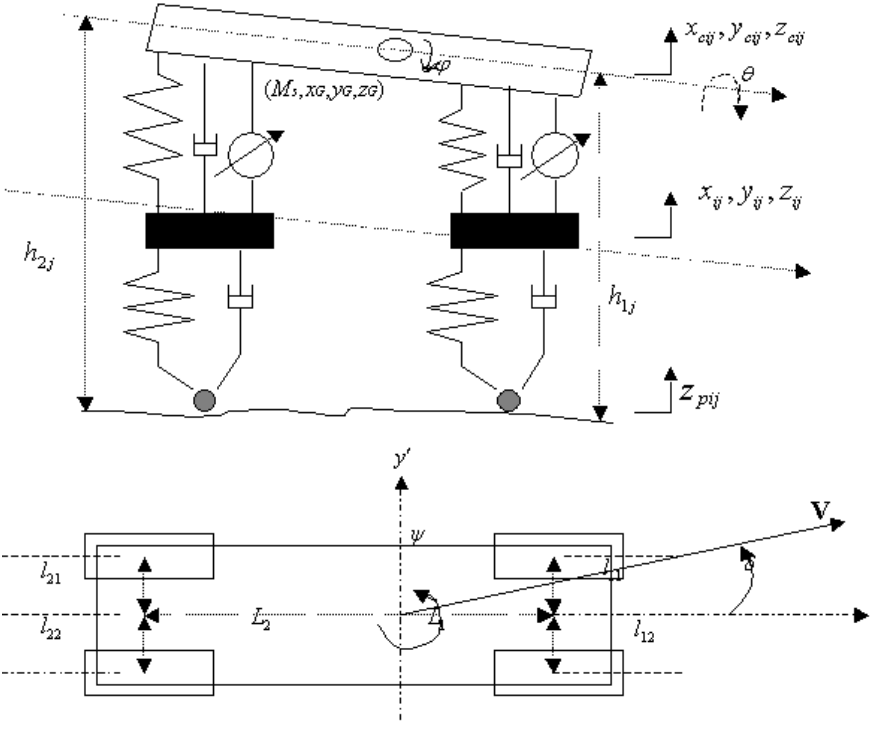

FIG. 3. Model of the complete vehicle.

2.2.1. Rigid mass of the vehicle. To determine the general equations of the model's movements in 3D, we used Lagrange equations [6]. Thus the equations of the vehicle's body are :

$$I_{x'x'}\frac{\partial^2\theta_G}{\partial t^2} = \sum_{i=1}^{2}(l_{i1}Fz_{i1} - l_{i2}Fz_{i2}) + \sum_{i,j=1}^{2} h_{ij}Fy_{ij} + M.g.h * \sin\theta, \tag{2.1}$$

$$I_{y'y'}\frac{\partial^2\varphi_G}{\partial t^2} = \sum_{j=1}^{2}(L_2Fz_{2j} - L_1Fz_{1j}) - \sum_{i,j=1}^{2} h_{ij}Fx_{ij}, \tag{2.2}$$

$$I_{z'z'}\frac{\partial^2\psi_G}{\partial t^2} = \sum_{i=1}^{2}(l_{i2}Fx_{i2} - l_{i1}Fx_{i1}) + \sum_{j=1}^{2}(L_1Fy_{1j} - L_2Fy_{2j}). \tag{2.3}$$

For the unsprung masses $(i, j = 1, 2)$, we can write:

$$M_{nsij}\ddot{z}_{ij} = -C_{sij}(\dot{z}_{ij} - \dot{z}_{cij}) - k_{sij}(z_{ij} - z_{cij}) - k_{pij}(z_{ij} - z_{pij}) - F_{aij}, \tag{2.4}$$

where F_{aij} represents the active force element to be controlled, F_{xij}, F_{yij} and F_{zij} represent the suspension forces under the wheels according to (Gx'),(Gy') and (Gz')axis of reference $R'(G, x', y', z')$ related to the vehicle mass center, C_{sij} represents the damping of the secondary suspensions, k_{si} and k_{pi} are respectively the stiffnesses of the secondary suspensions and the primary suspensions. $I_{x'x'}$, $I_{y'y'}$, $I_{z'z'}$ are respectively the inertias of the rigid body according to the axes of the $R'(G, x', y', z')$ reference related to the mass center of the vehicle. h_{1j} and h_{2j} are respectively the vertical distances from the ground to the axis of rolling at the front wheel-axle unit and the rear wheel-axle unit and h represents the vertical distance from the ground to the center of gravity of the unsprung mass. L_1 and L_2 are respectively the horizontal distances from the gravity center to the axis of rolling at the front wheel-axle unit and the rear wheel-axle unit and l_{ij} are the distances between the rolling axis and the vertical one which passes through the gravity center of each unsprung mass. M_s and M_{nsij} are respectively the masses of the rigid body and the unsprung masses ij. θ, φ and ψ are respectively the angle of roll, the angle of pitch and the angle of yaw of the rigid body. z_{pij} is the vertical road displacement and g is gravity.

The equations of the inertia center of the vehicle's movement which are obtained from the fundamental relation of dynamics are:

$$M.\ddot{x}_G - M.\dot{\psi}\dot{y}_G = \sum_{i,j=1}^{2} F_{xij}, \tag{2.5}$$

$$M.\ddot{y}_G + \dot{\psi}\dot{x}_G = \sum_{i,j=1}^{2} F_{yij}, \tag{2.6}$$

$$M.\ddot{z}_G = \sum_{i,j=1}^{2} F_{zij} - M * g, \tag{2.7}$$

with

$$M = M_s + \sum_{i,j=1}^{2} M_{nsij}.$$

The velocities of the gravity center in the reference R' are expressed by:

$$\begin{cases} \dot{x}_G = V.\cos\delta, \\ \dot{y}_G = V.\sin\delta, \end{cases}$$

and accelerations after linearization are:

$$\begin{cases} \ddot{x}_G = \dot{V}(1-\delta^2/2) - V\ \dot{\delta}\ \delta - \dot{\psi}\ V\delta, \\ \ddot{y}_G = \dot{V}\delta + V\ \dot{\delta} + \dot{\psi}\ V, \end{cases}$$

where δ represents the drift of the pneumatic and V represents the longitudinal velocity of the vehicle.

To study the vehicle's displacement in 3D, it is imperative to define a reference frame in which one will be able to consider the displacements in a straight line, but also the movements of yaw, pitch and roll. The selected references are: $R(\omega, x, y, z)$, the direct and fixed Galilean reference frame which is related to the ground reference frame. $R(G, x', y', z')$, the reference frame related to the mass center of the vehicle and obtained by rotation of angle ψ around the axis (G, z'). $R''(G, x'', y'', z'')$, the reference frame related to the mass center of the vehicle and obtained by rotation of angle φ around the axis (G, y''). And $R'''(G, x''', y''', z''')$, the reference frame related to the mass center of the vehicle and obtained by rotation of angle θ around the axis (G, x''').

The dynamic equations of the vehicle are established in the reference frame R'''. These equations are then expressed in the reference frame R, by using a matrix of passage P, linearized to the first order.

$$\mathbf{P} = \begin{pmatrix} 1 & -\psi & \varphi \\ \psi & 1 & -\theta \\ -\varphi & \theta & 1 \end{pmatrix}.$$

These equations are those of vehicle's body.

2.2.2. Wheels. The model of tyres used is a Pacejka model [7, 8], which allows the representation of tyre behaviour by taking account of the longitudinal/transverse coupling. The angles which we will refer to are those which are necessary for Pacejka's model and used for simulation. $(G,\ x_r,\ y_r,\ z_r)$ represents the reference frame of the wheel.

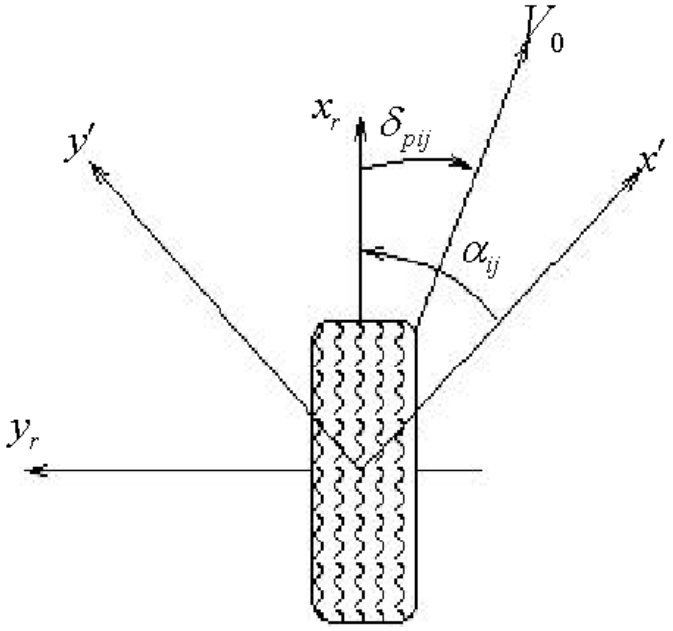

FIG. 4. Diagram of the tyre seen from above.

The pneumatic drifts (δ_{pij}) are expressed in the following way:

$$\delta_{pij} = \arctan\left(\frac{\vec{V}_0.\vec{y}_r}{\vec{V}_0.\vec{x}_r}\right) - \alpha_{ij} \tag{2.8}$$

where α_{ij} is the steering of the wheel's direction caused by the driver. The vertical efforts under each wheel are expressed in the following way

$$F_{zij} = -k_{pij}(z_{ij} - z_{pij}) - c_{pij}(\dot{z}_{ij} - \dot{z}_{pij}) + F_{zsij}, \tag{2.9}$$

where F_{zsij} is the static effort due to the load under each wheel. The forces given in the reference frame of each wheel are those of Pacejka's model. The passage of the efforts in the wheel reference frame to the frame R' is expressed as follows:

$$F_{xrij} = F_{xij}\cos\alpha_{ij} - F_{yij}\sin\alpha_{ij}, \tag{2.10}$$

$$F_{yrij} = F_{yij}\cos\alpha_{ij} + F_{xij}\sin\alpha_{ij}. \tag{2.11}$$

The pneumatic slip is defined by the following relation:

$$g = \begin{cases} \dfrac{(R.w - V) * 100}{V} & \text{if} \quad R.w < V, \\ \dfrac{(R.w - V) * 100}{R.w} & \text{if} \quad R.w > V. \end{cases} \tag{2.12}$$

All these equations enabled us to develop a software to simulate the road behaviour of a vehicle.

2.3. Description of the simulation software

The system is integrated in a simulation environment consisting of a complete model of the vehicle and is called VDS (Vehicle Dynamics Software). This model was developed by the structures and systems dynamics team of the Ecole Centrale de Lyon. This model enables simulation of the dynamic behaviour of a vehicle in real time, and thus allows experimentation on the frame using a control simulator, integrating the reactions of a real driver and the aerodynamics.

The model of tyre is also integrated in the tool for simulation and it takes account of the longitudinal/transverse coupling. The simulation tool was developed under MATLAB/Simulink.

3. Control laws developments

The objective of control is to find a suitable law to increase the normal force. We therefore minimize the vertical quadratic acceleration of the front and rear hubs and we limite the energy contribution necessary for control.

The parameters obtained for the front wheel on the 2D model is placed on the two front wheels of the 3D model. We proceed in the same way for the rear wheels. This is why the study of the control law was carried out on a 2D model.

The front and rear normal forces depend on movements in the vertical plane, which is the case of the displacements of the rigid body and the unsprung masses. We then separate the entry vector into two state vectors, one with the elements moving vertically and the other with the elements moving horizontally.

3.1. Model used

This model [9, 10, 11] of vehicle is composed of three rigid bodies. The suspended mass represents the rigid body and the two unsprung masses represent the front and rear axles. This model includes 9 (DOF) degrees of freedom: three degrees of freedom for the rigid body ($x,\ z,\ \theta$), two degrees of freedom for each unsprung mass ($x,\ z$), one degree of freedom for the rotation (w) of each wheel.

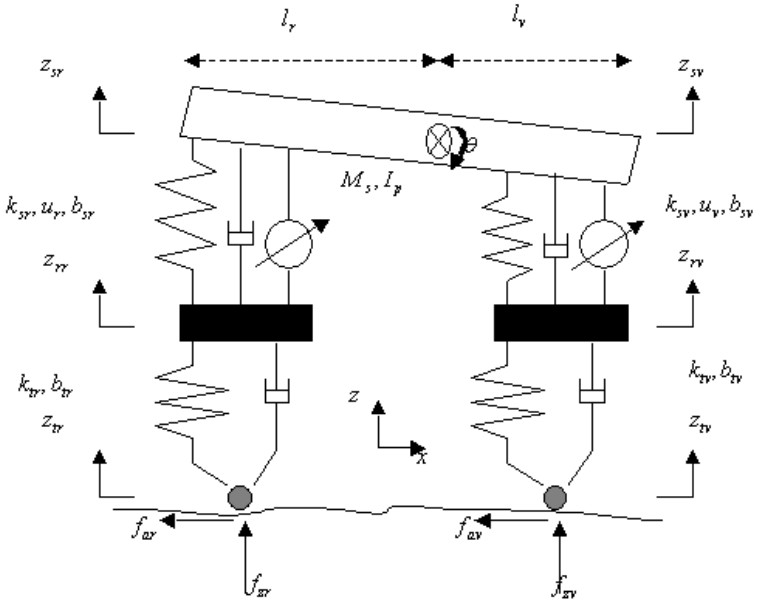

FIG. 5. Half car model.

The dynamic system can be expressed in the following form:

In the vertical plane,

$$\dot{Z} = A_1.Z + B_1.U + B_2(Z).F + B_3.W \tag{3.1}$$

with $A_1(8*8)$, $B_1(8*2)$, $B_2(8*2)$ as a function Z and $B_3(8*4)$.

In the horizontal plane,

$$\dot{X} = A_2.X + B_4.F + D.T \tag{3.2}$$

with $A_2(6*6)$,$B_4(6*2)$ and $D(6*2)$.

The vectors $\mathbf{X}$ and $\mathbf{Z}$ are:

$$\mathbf{X} = \begin{pmatrix} x \\ \dot{x} \\ w_{av} \\ \dot{w}_{av} \\ w_{ar} \\ \dot{w}_{ar} \end{pmatrix}, \qquad \mathbf{Z} = \begin{pmatrix} z_{sv} - z_{rv} \\ \dot{z}_{sv} \\ z_{rv} - z_{tv} \\ \dot{z}_{rv} \\ z_{sr} - z_{rr} \\ \dot{z}_{sr} \\ z_{rr} - z_{tr} \\ \dot{z}_{rr} \end{pmatrix}.$$

The choice of vectors was made for a suitable search for our control law, which constitutes an important stage of this study.

3.2. Expression of the criterion

The control law [12, 13] that we formulate is based on the minimization of a quadratic criterion for a linear dynamic system. This control provides the expression of the optimal forces according to the state variables of the system. Knowing the performance criterion and the equations of the system, we are able to identify the optimal forces to be applied for better road behaviour, regardless of the constraints related to the road state and the stochastic nature of the disturbances.

The variables to be minimized in our model are of two types: accelerations of the unsprung masses ($\ddot{z}_{rv}$ and $\ddot{z}_{rr}$), which would isolate the vehicle cockpit from irregularities in the road, thus making it possible to improve comfort of the passenger, and vertical displacements of the suspensions ($z_{sv} - z_{rv}$) and ($z_{sr} - z_{rr}$). To optimize the energy contribution necessary for the control forces, we have added the expressions J_5 and J_6 in the criterion of performance defined below. We define the criterion of performance as follows [14]:

J_1,J_2: being the quadratic evaluation of the front and rear accelerations respectively weighting the constants q_1 and q_2.

$$J_1 = \lim_{T\to\infty} \frac{1}{T}\, E \int_0^T q_1(\ddot{z}_{rv})^2 dt \tag{3.3}$$

$$J_2 = \lim_{T\to\infty} \frac{1}{T}\, E \int_0^T q_2(\ddot{z}_{rr})^2 dt \tag{3.4}$$

J_3,J_4: averages of squares of relative displacements between the rigid body and the axle, balanced respectively at the front and rear by the constants q_3 and q_4.

$$J_3 = \lim_{T\to\infty} \frac{1}{T}\, E \int_0^T q_3(z_{sv} - z_{rv})^2 dt \tag{3.5}$$

$$J_4 = \lim_{T\to\infty} \frac{1}{T}\, E \int_0^T q_4(z_{sr} - z_{rr})^2 dt \tag{3.6}$$

J_5,J_6: these terms are useful for limiting the control forces $u_v(t)$, $u_r(t)$ and thus controlling the strain energy of the suspension.

$$J_5 = \lim_{T\to\infty} \frac{1}{T}\, E \int_0^T \rho_v(u_v)^2 dt \tag{3.7}$$

$$J_6 = \lim_{T\to\infty} \frac{1}{T}\, E \int_0^T \rho_r(u_r)dt. \tag{3.8}$$

The coefficients ρ_v, ρ_r and q_i $(i = 1, ..., 4)$ are numerical constants whose values give predominance to one or the other of the performances to be achieved. The expression of the criterion will thus be

$$J = \sum_{i=1}^{6} J_i.$$

The square averages of these accelerations reveal a coupling and the index of performance can then be put in the form

$$J = \lim_{T\to\infty} \frac{1}{T}\, E \int_0^T (U^T.R.U + X^T.Q.X + 2.X^T.N.U)dt. \tag{3.9}$$

with

$$\mathbf{Q} = \begin{pmatrix} q_3 + q_1.a_1^2 & a_1.a_2.q_1 & a_1.a_3.q_1 & a_1.a_4.q_1 & 0 & 0 & 0 & 0 \\ a_1.a_2.q_1 & q_1.a_2^2 & a_2.a_3.q_1 & a_2.a_4.q_1 & 0 & 0 & 0 & 0 \\ a_1.a_3.q_1 & a_2.a_3.q_1 & q_1.a_3^2 & a_3.a_4.q_1 & 0 & 0 & 0 & 0 \\ a_1.a_4.q_1 & a_2.a_4.q_1 & a_3.a_4.q_1 & q_1.a_4^2 & 0 & 0 & 0 & 0 \\ 0 & 0 & 0 & 0 & q_4 + q_2.a_5^2 & a_5.a_6.q_2 & a_5.a_7.q_2 & a_5.a_8.q_2 \\ 0 & 0 & 0 & 0 & a_5.a_6.q_2 & q_2.a_6^2 & a_6.a_7.q_2 & a_6.a_8.q_2 \\ 0 & 0 & 0 & 0 & a_5.a_7.q_2 & a_6.a_7.q_2 & q_2.a_7^2 & a_7.a_8.q_2 \\ 0 & 0 & 0 & 0 & a_5.a_8.q_2 & a_6.a_8.q_2 & a_7.a_8.q_2 & q_2.a_8^2 \end{pmatrix},$$

$$\mathbf{R} = \begin{pmatrix} \rho_v + q_1.a_{10}^2 & 0 \\ 0 & \rho_r + q_2.a_9^2 \end{pmatrix}, \qquad \mathbf{N} = \begin{pmatrix} a_1.a_{10}.q_1 & 0 \\ a_1.a_{10}.q_1 & 0 \\ a_1.a_{10}.q_1 & 0 \\ a_1.a_{10}.q_1 & 0 \\ 0 & a_5.a_9.q_2 \\ 0 & a_5.a_9.q_2 \\ 0 & a_5.a_9.q_2 \\ 0 & a_5.a_9.q_2 \end{pmatrix},$$

$$a_1 = -ksv/M_{nsv}; \qquad a_6 = -bsr/M_{nsr};$$
$$a_2 = -bsv/M_{nsv}; \qquad a_7 = -ktr/M_{nsr};$$
$$a_3 = -ktv/M_{nsv}; \qquad a_8 = (bsr - btr)/M_{nsr};$$
$$a_4 = (bsv - btv)/M_{nsv}; \qquad a_9 = 1/M_{nsr};$$
$$a_5 = -ksr/M_{nsr}; \qquad a_{10} = 1/M_{nsv}.$$

The values used in the calculation of the criterion are given below [15]:

$$M_s = 730.0 \text{ kg}, \qquad I_p = 1230.0 \text{ kg.m}^2,$$
$$r = 0.3 \text{ m}, \qquad J_v = 1.4 \text{ kg.m}^2,$$
$$J_r = 1.0 \text{ kg.m}^2, \qquad k_{sv} = 19960.0 \text{ N/m},$$
$$k_{sr} = 17500.0 \text{ N/m}, \qquad b_{sv} = 1050.0 \text{ N.s/m},$$
$$b_{sr} = 900.0 \text{ N.s/m}, \qquad l_v = 1.011 \text{ m},$$
$$l_r = 1.803 \text{ m}, \qquad h = 0.508 \text{ m},$$
$$M_{nsv} = 40.0 \text{ kg}, \qquad M_{nsr} = 35.0 \text{ kg},$$
$$k_{tv} = 175500.0 \text{ N/m}, \qquad k_{tr} = 175500.0 \text{ N/m},$$
$$b_{tv} = 1500.0 \text{ N.s/m}, \qquad b_{tr} = 1500.0 \text{ N.s/m}.$$

The determination of the elements $u_v(t)$ and $u_r(t)$ and the law of control consists of finding the matrix which is the solution of the Riccati equation below:

$$P(t).A_1 + A_1^T.P(t) + Q - P(t).B_1.R^{-1}.B_1^T.P(t) = 0 \tag{3.10}$$

where P, Q and R are defined, symmetrical and positive matrices. The command which minimizes this criterion of performance is :

$$U(Z,t) = G(t).Z(t) \quad with \quad G(t) = -R^{-1}.B_1^T.P(t) \tag{3.11}$$

Elements $u_v(t)$ and $u_r(t)$ are written in the form:

$$\begin{pmatrix} u_v \\ u_r \end{pmatrix} = G.Z.$$

Generally, the development of a suspension is a compromise between the minimization of two variables (acceleration and vertical displacement), but the minimization of vertical displacement does not appear on the same level. So the choice of the ponderation coefficients, and thus of the optimal law, determines the control performance. As there is no suitable criterion for determining the

parameters, their adjustment is thus made in a dichotomic way. For the law of control, we choose the ponderation coefficients with the following values:

$$\rho_v = 1.75.10^{-9}, \quad \rho_r = 1.75.10^{-9},$$
$$q_1 = 10^{-8}, \quad q_2 = 10^{-8}, \quad q_3 = 0.9, \quad q_4 = 2.1,$$

We then examine the shape of the curves to decide on the effectiveness of the law of control.

4. Simulation

Active suspension control is intended to help the driver to deal with extreme driving situations generally leading to a loss of control of the vehicle, and thus an accident. Extreme situations targeted by a trajectory control system are for light vehicles, in the case of under and over-steering. The system equipped with an active suspension has to keep the vehicle on its trajectory, materialized by the steering wheel and guided by the driver. The command law synthesized in the previous paragraph was integrated on a vehicle. Among the emergency situations studied, we present the one which consists of avoiding an obstacle and then we will compare the behaviour of the active suspension-equipped vehicle with the behaviour of the one without such a system.

4.1. Skirting–cutting in

In the following, simulations correspond to the voluntary behaviour of the driver when an obstacle suddenly appears, as shown below (Fig. 6). The vehicle rolls at a speed of 130 km/h. On seeing the obstacle, the driver brakes one second later, steering the driving wheel to the left at a 60 degrees angle, then steers back to put the vehicle on its initial trajectory again.

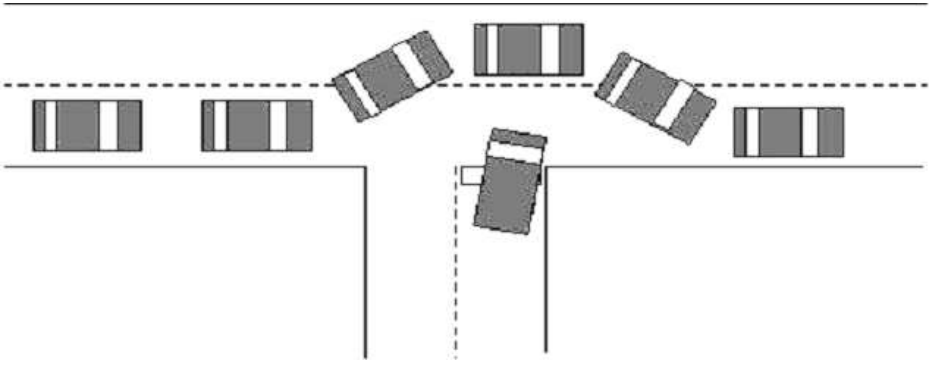

Fig. 6. The driver's maneuver.

During maneuvering the driver keeps his foot on the brake. This occurs with good grip corresponding to a dry road. The results obtained for vertical suspension control (as shown in Figures b) are compared with those without control (as shown in Figures a).

4.2. Results

Responding automatically to the driver's instruction, the vehicle is decelerated by pressing the brakes to around -9 m/s^2. This strong deceleration happens abruptly and leads to a loss of grip. The loss of grip decreases the braking. This leads to a loss of longitudinal deceleration (γ_x) after 3 seconds (Fig. 7a) in favour of acceleration (γ_y). While in Fig. 7b, the longitudinal deceleration (γ_x) of the controlled vehicle holds until the end of the maneuvering and the side acceleration is near zero after 3.5 seconds. Under these conditions, the vehicle equipped with active suspensions will follow the desired trajectory more easily and its wheels will transmit the lateral effort to the ground.

When the driver steers the wheel to the left, a lateral load transfer occurs which tends to unload the left-hand front and rear wheels in favour of the right-hand front and rear wheels. And braking generates a transfer of longitudinal load from the rear wheels to the front ones. The left rear wheel, unloaded from a large share of its load, is then on the verge of losing contact with the road. This wheel cannot therefore transmit any effort to the ground and for severe decelerations (> -8 m/s^2), it quickly locks (Fig. 8a).

The right-hand rear wheel, partly unloaded from its load by the longitudinal transfer, also locks equally during the braking phase. The wheel cannot compensate the transversal effort lost at the level of the left rear wheel.

With the deceleration imposed by the driver of the non-controlled vehicle, the longitudinal transfer generates an additional overload on the right front wheel which saturates completely. Longitudinal friction forces are thus stronger (Fig. 11a). The left front wheel unloaded during the turn receives the same braking order as the right front wheel. Under these conditions, the left front wheel blocks itself quite quickly ($slipping = -100\%$) and thus cannot transmit any lateral effort. The right front wheel, saturated and greatly longitudinally stressed, cannot provide enough lateral effort to compensate the blocking of the left front wheel. All four wheels are then blocked (Fig. 8a).

The active force synthesized by the control law and drawn in Fig. 8c, instantly balances the load of the suspended mass by adding an additional load when a wheel becomes unloaded, and by releasing the wheel when it is saturated.

Through its action, the active force allows the left front and rear wheels to return to a slip value (-10%) easing the driver's maneuvering.

a)

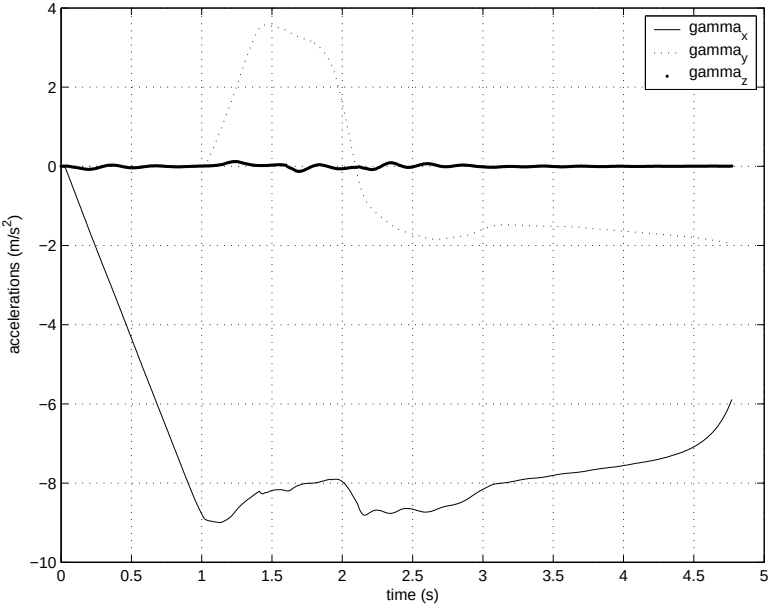

b)

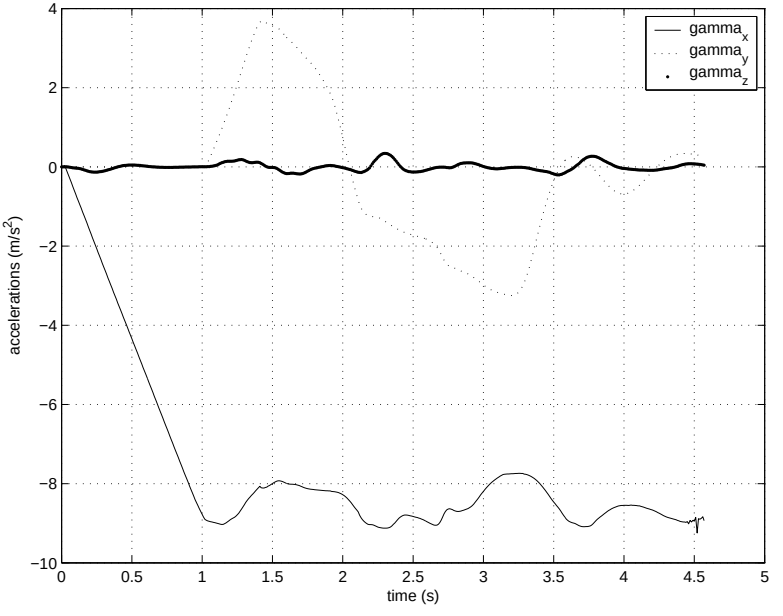

FIG. 7. a) Accelerations of non-controlled vehicle; b) Accelerations of controlled vehicle.

a)

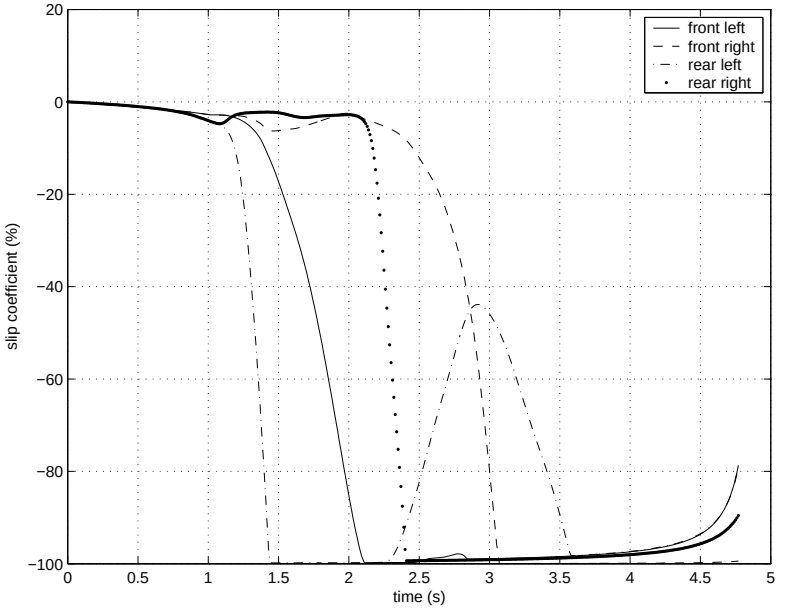
front left
front right
rear left
rear right
slip coefficient (%)
time (s)
20
0
−20
−40
−60
−80
−100
0
0.5
1
1.5
2
2.5
3
3.5
4
4.5
5

b)

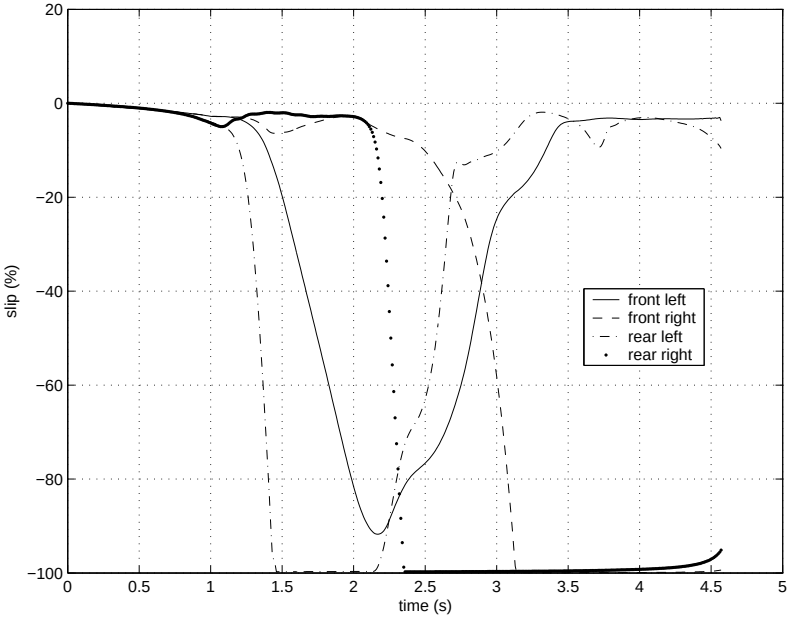
front left
front right
rear left
rear right
slip (%)
time (s)
20
0
−20
−40
−60
−80
−100
0
0.5
1
1.5
2
2.5
3
3.5
4
4.5
5

[Fig. 8a,b].

c)

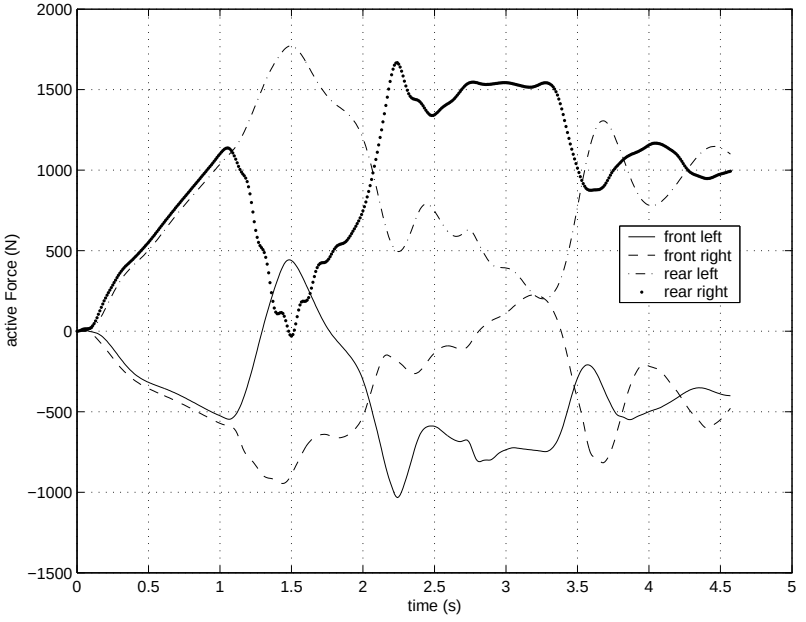

FIG. 8. a) Slip coefficient of non-controlled vehicle; b) Slip coefficient of controlled vehicle; c) Active force

Figure 9a shows the roll, pitch and yaw angles of the uncontrolled vehicle and Fig. 9b displays the same angles for the controlled vehicle. The roll on the controlled vehicle is lower than on the non-controlled one. This result means that the lateral load transfer is lower on our controlled vehicle. It is also the case for pitch which is lower on the controlled vehicle. This decreases the longitudinal load transfer. The front wheels will thus be less loaded and the rear ones less unloaded. The reduction of roll and pitch increases the vehicle stability, makes it more confortable and enables better braking thanks to better distribution of the load on the wheels.

When we analyze the rotation around axis (Gz) during the maneuver, the controlled vehicle has less yaw at the end of the maneuver, than the vehicle without control. This means that the non-controlled vehicle is far from the initial direction of its movement. The driver will have more difficulty putting his vehicle back to its initial direction. This generates a large lateral drift of the vehicle's center of gravity (Fig. 10a). Whereas the controlled vehicle has a lower drift angle at the center of gravity (Fig. 10b). It will be easier for the driver in this case to return to the initial direction of his movement.

a)

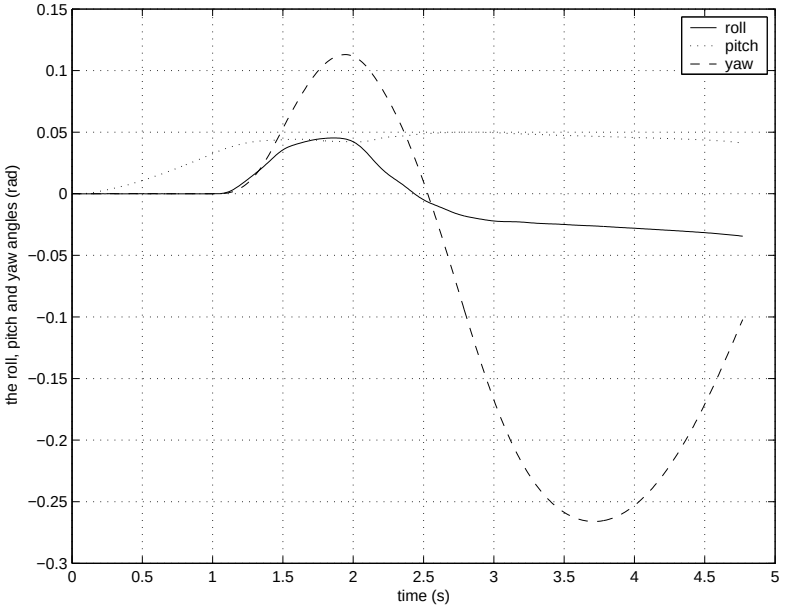

b)

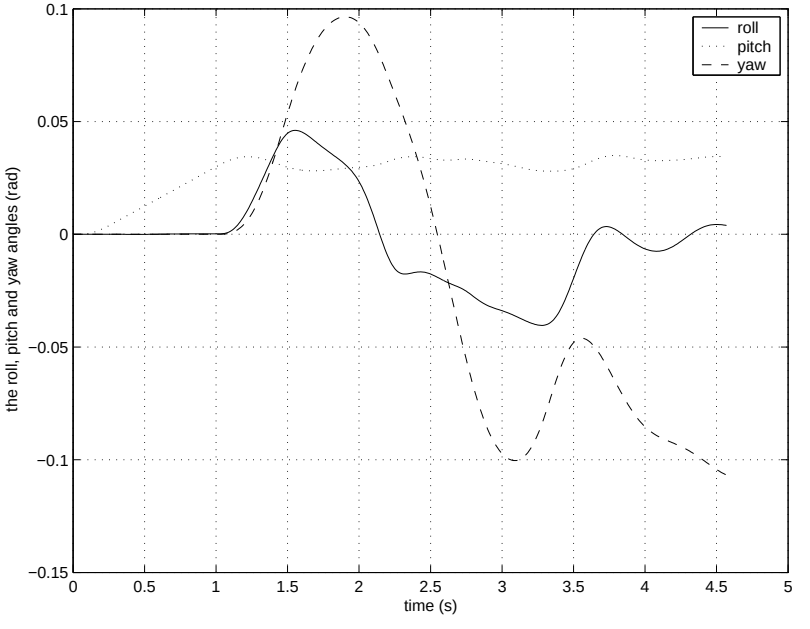

FIG. 9. a) Angles of non-controlled vehicle; b) Angles of controlled vehicle.

a)

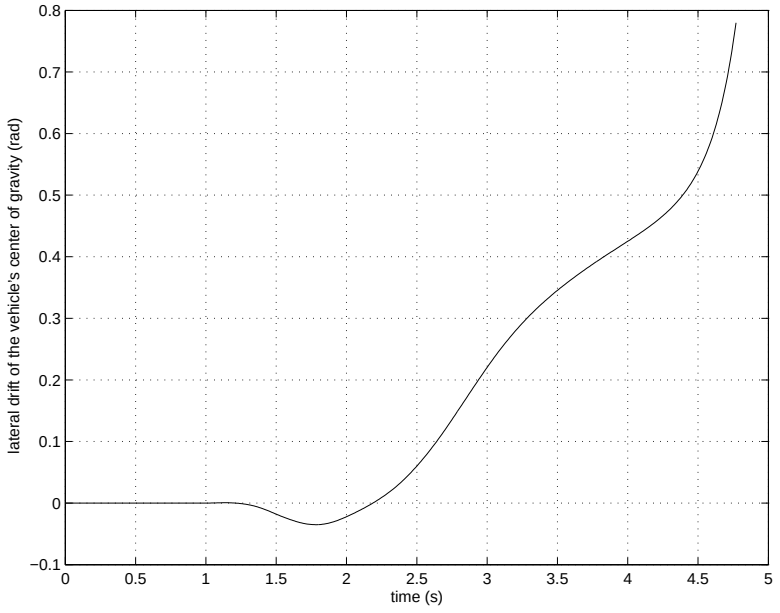

b)

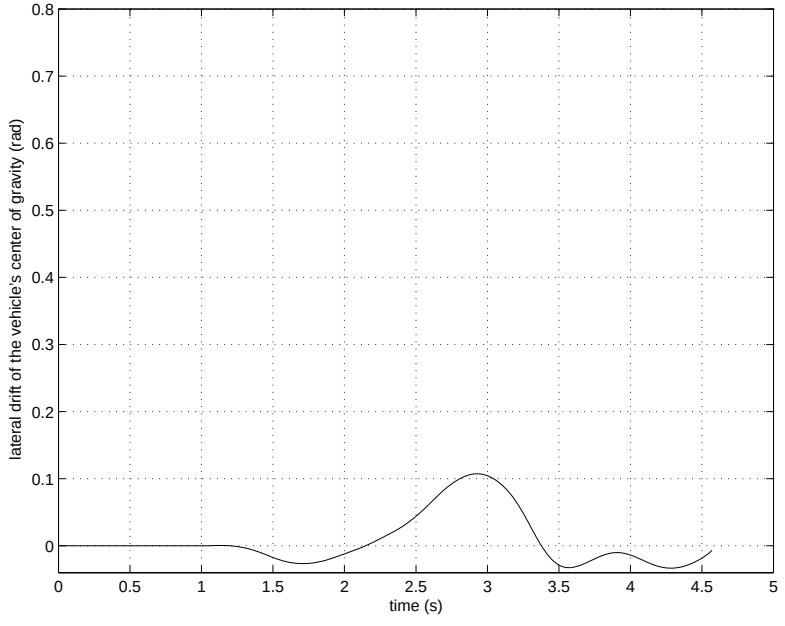

FIG. 10. a) Non-controlled vehicle: lateral drift of vehicle's center of gravity; b) Controlled vehicle: lateral drift of vehicle's center of gravity.

Longitudinal transfer during braking saturates the front wheels and unloads the rear ones. Furthermore, light vehicle manufacturers tend to load the front more than the rear. The friction of the front wheels becomes greater than that of the rear wheels (Fig. 11a and Fig. 11b).The exponential increase of drift at the center of gravity and the locking of the wheels of the non-controlled vehicle lead to an important loss of friction forces of the front wheels (Fig. 11a).

In Fig. 11b it can be seen that the longitudinal braking of the controlled vehicle is not decreased. This is caused by a decrease of the slip of the left front wheel and also to a hold of the transverse acceleration at around 0 $\mathrm{m/s^2}$.

For the vehicle without control, all wheels are locked, the center of gravity drift is high and the longitudinal deceleration is impaired. Under these conditions, the vehicle will have great difficulty responding to the driver's orders. The controlled vehicle holds its longitudinal deceleration until the end of the maneuver. Moreover, the drift at the center of gravity is lower than in the case of the non-controlled vehicle. The left front and rear wheels do not lock and so they compensate the locking of the two other wheels to ensure the trajectory desired by the driver.

In Fig. 12, the trajectories seen in the two previous cases are superposed.

The non-controlled vehicle cannot respond to the driver's orders. It moves 4 m sideways, which can cause it to leave the road. Whereas the controlled vehicle perfectly follows the desired trajectory.

a)

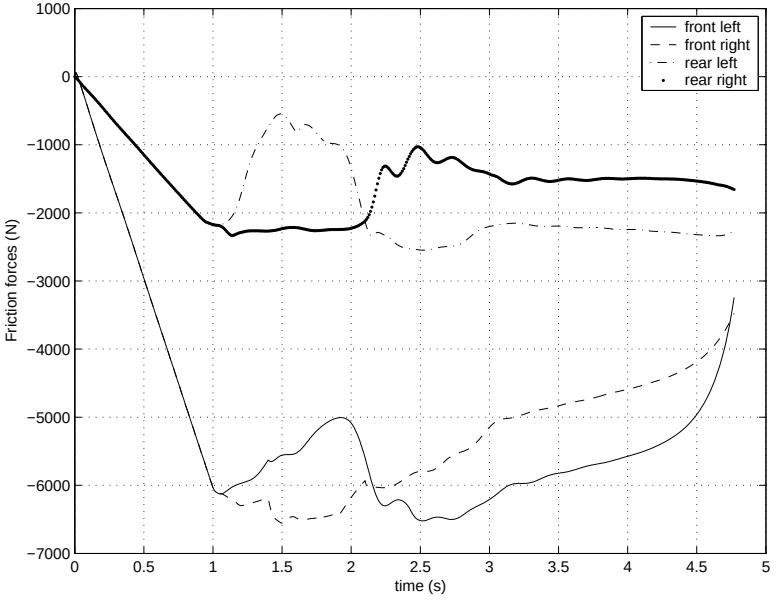

[Fig. 11a].

b)

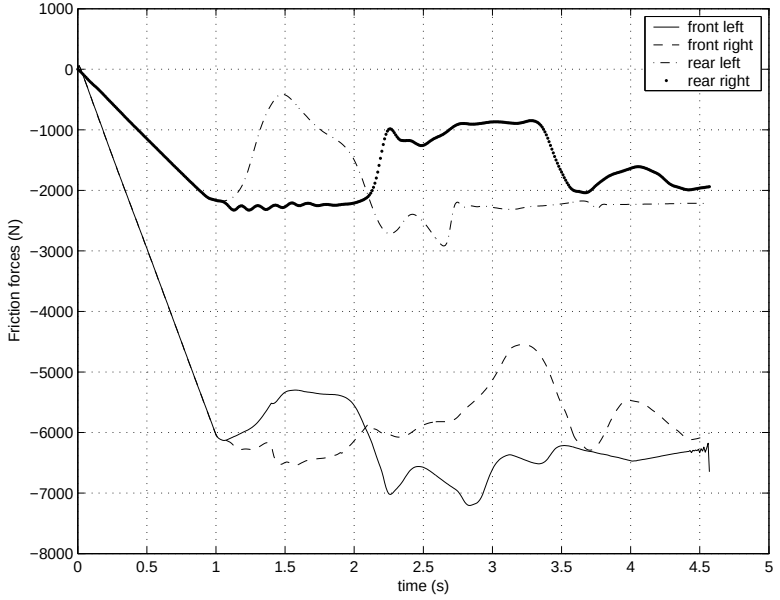

FIG. 11. a) Friction forces of non-controlled vehicle; b) Friction forces of controlled vehicle.

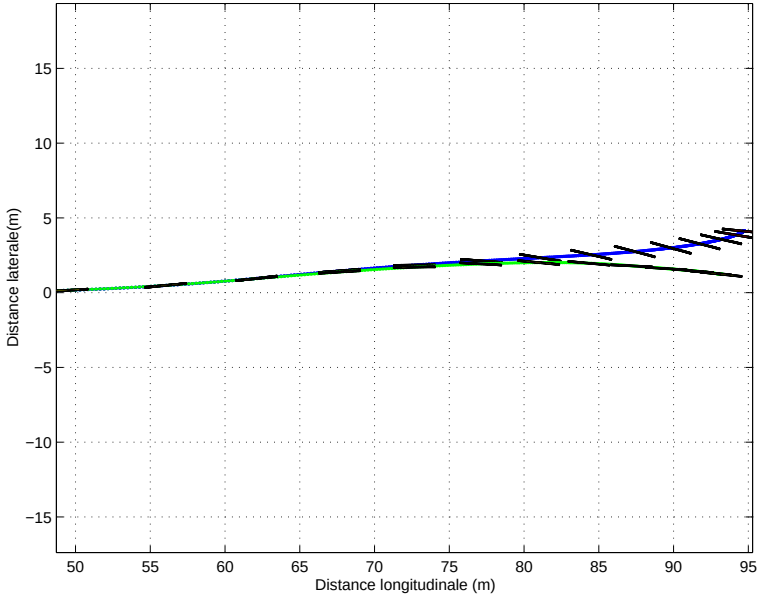

FIG. 12. Vehicle's trajectories.

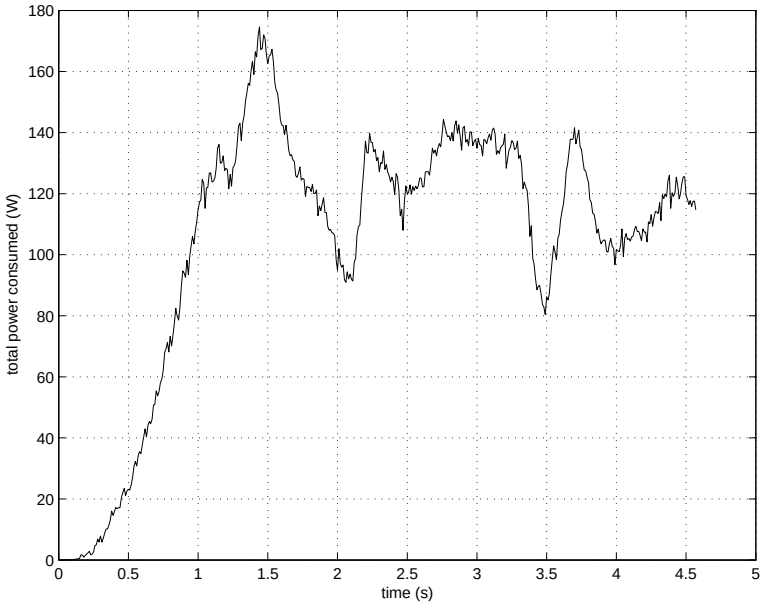

Fig. 13. Total power consumed.

Figure 13 shows the total instant power consumed by the four wheels during the maneuver.

It never exceeds 200 W, what is very reasonable. Energy consumption is a primary factor if the system is to be put in use because current vehicles occasionally have high consumption levels. A system adding greatly to energy consumption has little chance of acceptance.

Many maneuver simulations have been conducted, notably while turning or driving in a straight line. The results of all these trials show that the controlled suspension system gives a better trajectory hold and better respect of the angle order of the steering wheel, with low friction, which is a clear ad-vantage.

5. Conclusion and perspectives

In this study we have analyzed, modelled and simulated an active suspension to improve the traction of a car during the braking phase.

Our margin for obtaining satisfying results was limited. Indeed today's tyres are employed at around 95% of their maximum efficiency. As tyres are designed to endure up to 110% of their capability, we can add a reasonable supplementary load.

From the general results of the optimization, an active command law on a nonlinear system was synthesized. As these theoretical laws are only rarely applied to real systems, we had to devise the control strategies integrating the technological constraints linked to the structure control. For example, taking into account the energy failure for the control of some structures, considering the measurability of states or ascertaining the stability and observability of the systems to be controlled. A control law was validated on the numerical model of real structures in the field of automotive suspensions.

For a good description of a vehicle on the verge of slip, it appears necessary to use a non-linear tyre model and a description of the vehicle taking into account at least the longitudinal and lateral speeds, the yaw, pitch accelerations, the rotations of the four wheels and the maximum side slip of the tyres.

In this study, we have obtained an improvement of traction thanks to piloted suspensions. This was done without any loss of comfort. A numerical study consisting of associating these piloted suspensions with existing active safety systems (ABS, ESP, ...) may be undertaken for application in the future vehicles.

References

1. D. Karnopp, M.J. Crosby, R.A. Harwood, *Vibration control using semi-active force generators*, ASME, Journal of Engineering for Industry Transport, 2–8, 1974.
2. D. Karnopp, S.G. So, *Energy flow in active attitude control suspensions: a bond graph analysis*, Vehicle System Dynamics, **29**, 69–81, 1998.
3. H.E. Tseng, J.K. Hedrick, *Semi-active control laws – optimal and sub-optimal*, Vehicle System Dynamics, **23**, 1994.
4. O. Yaniv, *Robustness to speed of 4WS vehicles for yaw and lateral dynamics*, Vehicle System Dynamics, **27**, 221–234, 1997.
5. D.E. Williamsand W.M. Haddad, *Active suspension to improve vehicle ride and handling*, Vehicle System Dynamics, **28**, 1–24, 1997.
6. A. Gentile, A. Messina, A. Trentadue, *Dynamic behaviour of a mobile robot vehicle with a two caster and two driving wheel configuration*, Vehicle System Dynamics, **25**, 89–112, 1996.
7. E. Bakker, H.B. Pacejka, L. Lidner, *A new tire model with and application in vehicle dynamics studies*, SAE paper No 890087, 1989.
8. E.J.H de Vries, H.B. Pacejka, *Motorcycle tyre measurements and models*, Vehicle System Dynamics, **28**, 1998.
9. R.G. Langlois, R.J. Anderson, *Preview control algorithms for the active suspension of an off-road vehicle*, Vehicle System Dynamics, **24**, 65–97, 1995.
10. E. Esmailzadeh, F. Fahimi, *Optimal adaptative active suspensions for a full car model*, Vehicle System Dynamics, **27**, 89–107, 1997.

11. D.C. Rutledge, M. Hubbard D. Hrovat, *A two DOF model for jerk optimal vehicle suspensions*, Vehicle System Dynamics, **25**, 113–136, 1996.

12. P. de Larminat, *Automatique - commande des systems linéaires*, Hermes.

13. A.G. Thompson P.M. Chaplin, *Force control in electrohydraulic active suspensions*, Vehicle System Dynamics, **22**, 1993.

14. T.R. Ori, *Suspensions actives et comportement dynamique des véhicules lors du freinage*, PHD Thesis n°2001-23, Ecole Centrale Lyon, 2001.

15. A. Alleyne, *Improved Vehicle performance using combined suspension and braking forces*, Vehicle System Dynamics, **27**, 235–265, 1997.

Received March 20, 2006.